Anoxic photochemical oxidation of siderite generates molecular hydrogen and iron oxides

J. Dongun Kim[a], Nathan Yee[b,c], Vikas Nanda[d], and Paul G. Falkowski[a,b,c,e,1]

Departments of [a]Chemistry and Chemical Biology, [b]Environmental Sciences, and [c]Earth and Planetary Sciences, Rutgers University, Piscataway, NJ 08854; [d]Department of Biochemistry, Robert Wood Johnson Medical School, University of Medicine and Dentistry of New Jersey, Piscataway, NJ 08854; and [e]Institute of Marine and Coastal Sciences, Rutgers University, New Brunswick, NJ 08901

Contributed by Paul G. Falkowski, May 10, 2013 (sent for review April 24, 2013)

Photochemical reactions of minerals are underappreciated processes that can make or break chemical bonds. We report the photooxidation of siderite ($FeCO_3$) by UV radiation to produce hydrogen gas and iron oxides via a two-photon reaction. The calculated quantum yield for the reaction suggests photooxidation of siderite would have been a significant source of molecular hydrogen for the first half of Earth's history. Further, experimental results indicate this abiotic, photochemical process may have led to the formation of iron oxides under anoxic conditions. The reaction would have continued through the Archean to at least the early phases of the Great Oxidation Event, and provided a mechanism for oxidizing the atmosphere through the loss of hydrogen to space, while simultaneously providing a key reductant for microbial metabolism. We propose that the photochemistry of Earth-abundant minerals with wide band gaps would have potentially played a critical role in shaping the biogeochemical evolution of early Earth.

photogeochemistry | Archean iron cycle | astrobiology | banded iron formations

In the early Archean eon, mineral surfaces have been hypothesized to have played a significant role in adsorbing and concentrating biologically relevant molecules and carrying out various chemical reactions as catalysts or reactants (1–4). Upon exposure to a flux of photons, minerals may undergo photoinduced electron excitation reactions, driving electron transitions, such as crystal field transitions, valence and conduction band transitions, and molecular orbital transitions as intervalence charge transfer (5). As a result, the photochemical reactions of minerals potentially can influence chemical reactions of basic elements such as H, C, N, and O. Over geologic time scales, the fluxes of major chemical elements would have cycled through such photochemical reactions, before biological chemistry of life on Earth (6). We hypothesize that emergent photogeochemical cycles may have played a critical role in shaping the early Earth environment.

In this article we examine the potential photochemical reactions of siderite in the production of molecular hydrogen. Although gaseous hydrogen is virtually nonexistent in the contemporary atmosphere, in the early Archean the gas would have enhanced the greenhouse effect directly (7) and indirectly extended the lifetime of atmospheric methane. Both processes would have helped water to remain liquid on Earth's surface despite significantly lower solar luminosity. Further, the existence of a hydrogen-rich environment would have enabled the spontaneous synthesis of key building blocks of life (1), and served as an electron donor in the early evolution of microbial metabolism (8). Despite its importance, the details of the early Archean hydrogen cycle are poorly understood.

Photochemical origins of molecular hydrogen have been proposed previously (9–12). The reactions suggested were based on the photooxidation of reduced metal species, such as hydrated Fe(II). Indeed, previous studies have confirmed this type of reaction; however, the ferrous iron species used (10–12) are unlikely to have been present in the upper ocean in the early Archean (13) because the precipitation of Fe(II) minerals would have been rapid. Instead, the major ferrous species in the early Archean upper ocean with a relatively low sulfide concentration would most likely have been associated with silicates and carbonate minerals such as siderite ($FeCO_3$), depending primarily on the pCO_2 level (14).

Models of Earth's early atmosphere also suggest the presence of very high concentrations of CO_2 (15). One consequence of high concentrations of CO_2 in contact with an anoxic, ferruginous ocean would be the spontaneous precipitation of siderite with an experimentally determined solubility product (K_{sp}) of $\sim 10^{-10}$ (16). In the absence of oxygen, siderite precipitates through the reaction of ferrous iron with dissolved inorganic carbon (HCO_3^-, CO_3^{2-}); this reaction would have been thermodynamically highly favorable in the Archean. Indeed, siderite is found in rocks as old as 3.8 Ga, and its abundance suggests it was a prevalent ferrous species during Archean time (17–21). Although UV photooxidation of siderite is possible (22), and may have implications for the early hydrogen cycle, the rates and mechanisms of hydrogen production by this potential geochemical pathway have not been experimentally elucidated.

Here we report a reaction of UV photons with siderite that generates molecular hydrogen and iron oxides under anoxic conditions.

Results

Photochemical Oxidation of Siderite. To examine the potential photochemical reaction of siderite, we synthesized and suspended the mineral in anoxic aqueous phase and irradiated it with broadband light from a Xe source. Over a period of 24 h, the grayish white mineral became brown (Fig. 1), and upon further irradiation, a black/dark brown product was formed. The product was magnetic (Fig. 2*A*) and X-ray diffraction analysis confirmed it had a spinel structure concordant with either magnetite and/or maghemite (Fig. 2*B*). Measurements of the headspace revealed the presence of hydrogen gas. Mass spectroscopy and control experiments confirmed that the production of hydrogen resulted from a photochemical reaction with siderite.

To determine the effective absorption cross-section of the reaction, we isolated the spectral irradiance with bandpass filters. We assumed the effective cross-section of siderite photooxidation, $\Phi(\lambda)$, follows a Gaussian distribution with a function:

$$\Phi(\lambda) = e^{\frac{(\lambda-\lambda_{max})^2}{\sigma^2}}, \quad [1]$$

where λ_{max} is the wavelength at maximal effective absorption cross-section. The irradiance spectrum from the Xe source through a filter, $I(\lambda)$, multiplied by $\Phi(\lambda)$ yields an effective absorption spectrum. The integrated area under $I(\lambda)\times\Phi(\lambda)$ is proportional to the rate of hydrogen evolution (Fig. S1); hence, λ_{max} and σ can be

Author contributions: J.D.K. and P.G.F. designed research; J.D.K. performed research; J.D.K., N.Y., V.N., and P.G.F. analyzed data; and J.D.K., N.Y., V.N., and P.G.F. wrote the paper.

The authors declare no conflict of interest.

[1]To whom correspondence should be addressed. E-mail: falko@marine.rutgers.edu.

This article contains supporting information online at www.pnas.org/lookup/suppl/doi:10.1073/pnas.1308958110/-/DCSupplemental.

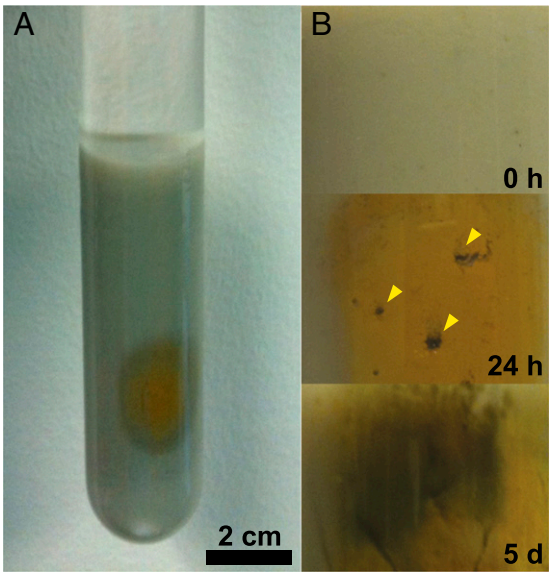

Fig. 1. (*A*) Siderite was placed in a quartz tube and irradiated with a Xe lamp with 300 W output under anoxic conditions at pH 7.5–8.0. (*B*) Siderite oxidation is observed as the color changes upon UV irradiation over time (from top to bottom). The mineral turns brown (oxyhydroxide) and subsequently black (magnetite). Trapped hydrogen bubbles are marked with yellow wedges.

solved numerically with three bandpass filters. Coarse-grained parameter fitting method was used with a step size of 0.1 for λ_{max} and 1 for variance (σ^2), and the least square fit was optimal with $\lambda_{max} = 267$ nm and $\sigma^2 = 123$. We determined the quantum yield for the reaction as the ratio of the number of hydrogen molecules produced to the number of photons absorbed by the siderite and the relative quantum yield follows the effective absorption cross-section of the reaction (Fig. 3*A*). To further elucidate the detailed reaction mechanism, we measured the amount of hydrogen produced under different light intensities. The experimental results (Fig. 3*B*) fit with a power function ($x^{2.08}$), revealing the rate of production of H_2 is proportional to the square of light intensity. The linear increase in quantum yield with increasing flux (Fig. 3*B*, *Inset*) strongly suggests the photochemical production of hydrogen requires two photons that drive two independent photochemical reactions.

Estimated Quantum Yield of the Photochemical Reaction Under Projected Archean Solar Flux. In the early Archean, the integrated solar flux was ~30% lower than present, but the relative contribution from UV radiation was proportionally higher and was not blocked by ozone (15). To estimate the solar UV flux, we used an estimated value of 0.1 W/m^2·nm (23). The UV photon flux from 245 to 290 nm, boundaries defined by the Gaussian curve (Fig. 3*A*), can then be calculated by (24):

$$\frac{Q(quanta \cdot m^{-2}\sec^{-1})}{W(watt \cdot m^{-2})} = \frac{\lambda}{hc} = \lambda(nm) \times 0.5035 \times 10^{16}, \quad [2]$$

which can be arranged:

$$Q(\lambda) = 0.5035 \times 10^{15} \times \lambda. \quad [3]$$

The integrated area under $Q(\lambda) \times \Phi(\lambda)$ yields the total number of effective UV photons per unit time (s) and area (m^2):

$$\int_{245}^{290} 0.5035 \times 10^{15} \times \lambda \times e^{\frac{(\lambda - \lambda_{max})^2}{\sigma^2}} d\lambda, \quad [4]$$

where λ_{max} is 267 nm and the variance (σ^2) is 123. The projected effective UV photon flux is 2.6×10^{18} quanta/m^2·s, or 4.4 μmol quanta/m^2·s. Because the photochemical oxidation of siderite is

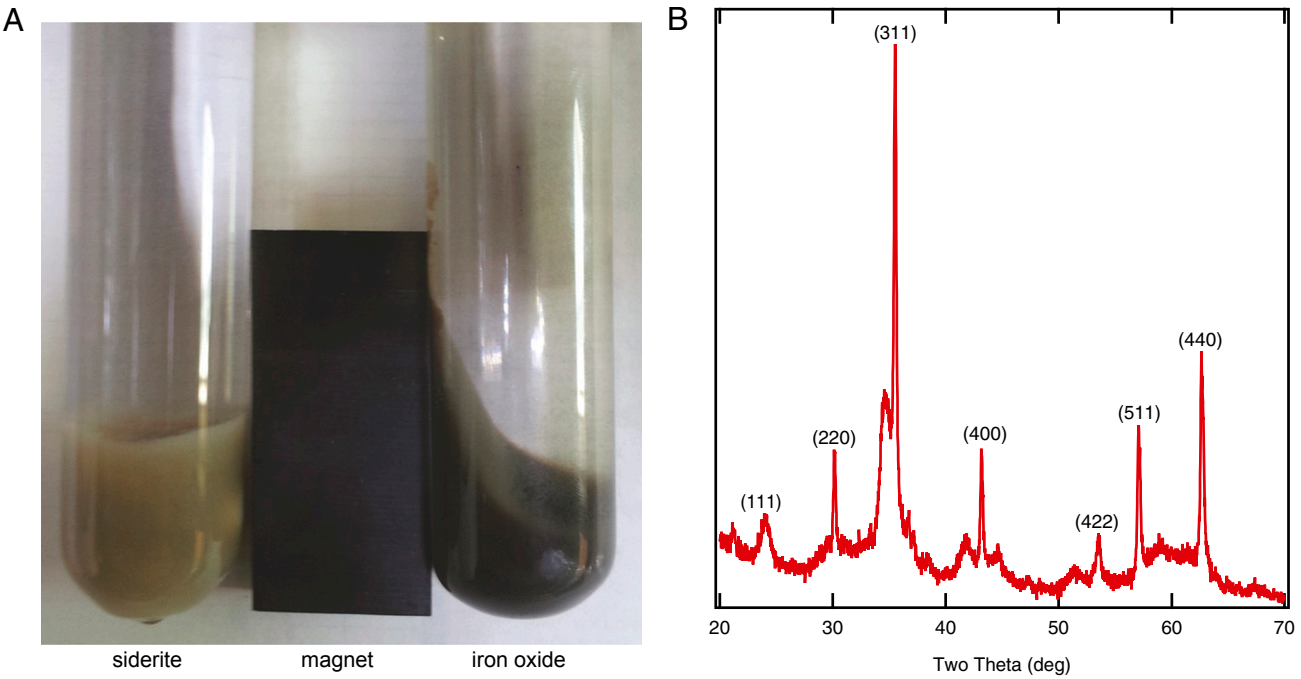

Fig. 2. (*A*) The photochemical oxidation of siderite (*Left*) leads to a magnetic product after 1 d of illumination under 600 W (*Right*). Upon exposure to oxygen, siderite readily becomes nonmagnetic goethite (Fig. S2 and S3). (*B*) Powder XRD spectra of the magnetic product reveals it is maghemite/magnetite under anoxic conditions.

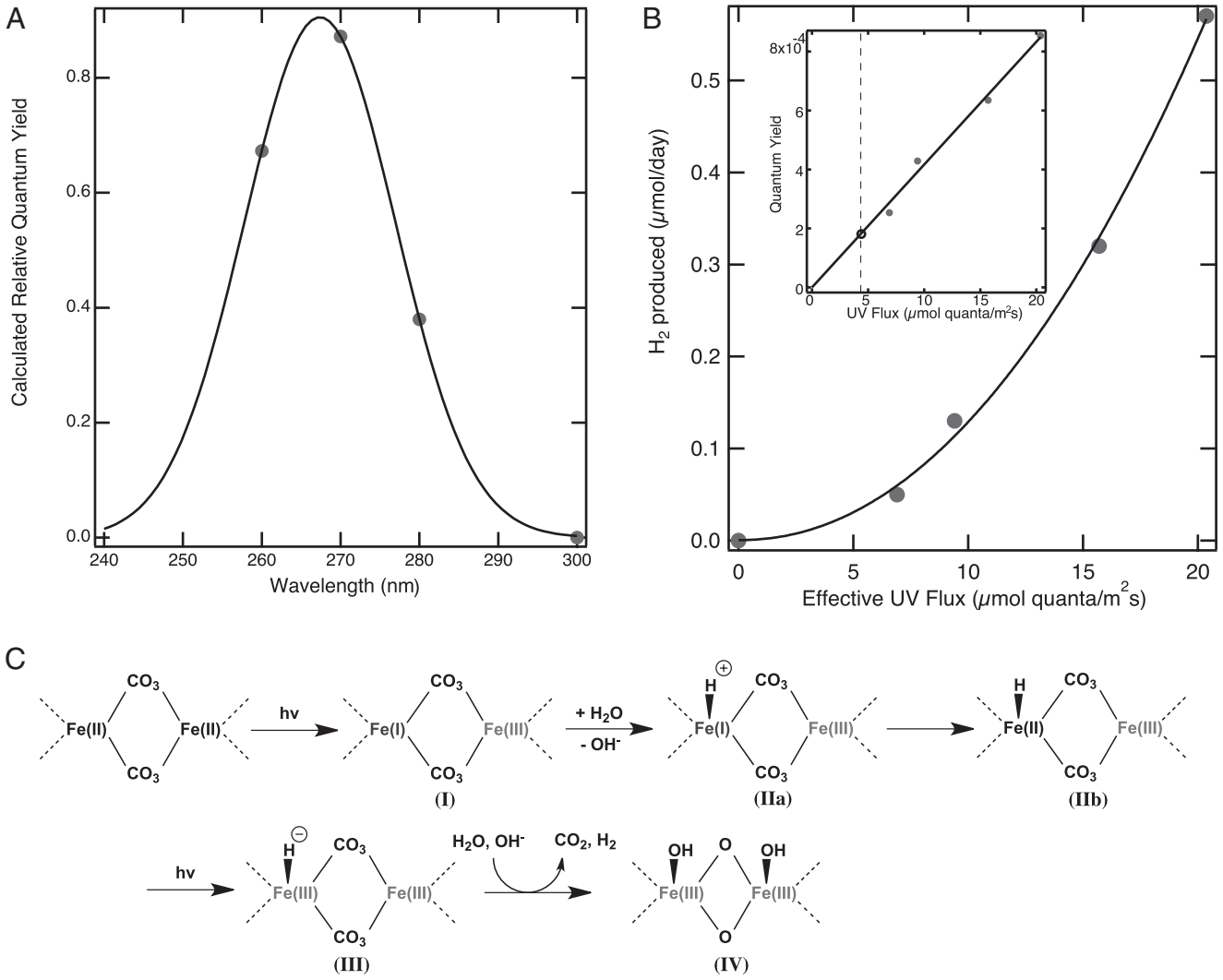

Fig. 3. (*A*) Plot of the relative quantum yield of the photochemical oxidation of siderite as a function of wavelength. The maximal cross-section is at 267 nm, which closely corresponds to the energy gap between the Fe(3d) ground state and a C–O antibonding orbital excited state. Four measurements were used to fit to a Gaussian function. (*B*) Plot of the hydrogen production (μmol) in 24 h as a function of the photon flux (μmol quanta/m^2·s). The experimental results revealed the rate of production of H_2 is proportional to the square of light intensity, and hence the yield increases linearly as a function of photon flux density. This analysis strongly suggests the overall reaction requires two photons to drive a two-electron transfer reaction mechanism. The estimated effective solar UV flux is ~4.4 μmol quanta/m^2·s at the ocean surface (dotted line) and the corresponding reaction yield based on the linear fit is $\sim 1.8 \times 10^{-4}$. (*C*) Proposed mechanism of the two-photon oxidation of siderite. Upon UV irradiation, an electron from Fe(3d) state is transferred to a neighboring iron atom generating charge separation (I). This process is probably assisted by intermediate product (IIa and IIb) by simultaneous protonation of surface Fe(I). A second photon oxidizes the intermediate product to hydrido–Fe(III), and this highly reactive intermediate product (III) reacts with a proton to form a molecular hydrogen. The two-photon reaction yields an Fe(III)–oxyhydroxide precursor (IV) after losing CO_2 and adding hydroxyl groups. Since two photons are involved in the reaction, the probability of H_2 production scales linearly with increasing flux.

a two-photon reaction, the linear increase in quantum yield with increasing flux suggests the effective quantum yield at the Earth's surface to have been $\sim 1.8 \times 10^{-4}$ (Fig. 3*B*).

Hydrogen Production Capacity in the Archean "Photic Zone." The attenuation coefficient at 270 nm through a water column is ~0.5 m^{-1} (25). Therefore, the flux at a given depth is reduced by a factor of $e^{-0.5x}$, where x is depth in meters. Based on the linear dependence of quantum yield to the photon flux density (Fig. 3*B*), we can estimate the H_2 production rate from a siderite surface at a given depth. Assuming a near-surface effective UV flux of 4.4 μmol quanta/m^2·s, the flux under x meters from the surface is $4.4 \times e^{-0.5x}$ μmol quanta/m^2·s. Since the reaction quantum yield is linearly proportional to the flux in μmol quanta/m^2·s with a slope of 4×10^{-5} (Fig. 3*B*), the H_2 production rate at x meters can be obtained as: $4.4e^{-0.5x} \times 4.4e^{-0.5x} \times 4 \times 10^{-5}$ μmol H_2/m^2·s.

Assuming the upper 1% of the ocean (~40 m) was the "photic zone," we can estimate the hydrogen production in μmol/m^{2}s based on the estimated quantum yield and UV photon flux, both in μmol/m^2·s.

$$\int_0^{40} (QY \times flux)\, dx = \int_0^{40} \left(4 \times 10^{-5} \times 4.4e^{-0.5x} \times 4.4e^{-0.5x}\right) dx \approx 7.74 \times 10^{-4}. \quad [5]$$

Hence, the estimated maximum hydrogen production capacity in the upper 1% of the Archean ocean was $\sim 7.7 \times 10^{-4}$ μmol H_2/m^{2}s. With 510,100,000 km^2 surface area on Earth, of which 40% (80%

ocean, of which half is exposed to the sun at any given time) can produce iron oxides, the estimated maximum iron oxide production capacity is estimated to be $\sim 10^{13}$ mol/y. However, the actual hydrogen flux from the photooxidation would almost certainly be limited by the amount of reduced iron species.

Global Significance of Hydrogen and Iron Oxide Production from Photochemical Reaction. The main sources of iron to the Archean ocean were hydrothermal vents and subaerial volcanoes. Given a flux of water through hydrothermal systems of 3×10^{13} kg/y in the contemporary ocean (26), and provided the hydrothermal flux was ~3 times higher in the Archean (27), the Archean hydrothermal water flux is estimated to be $\sim 9 \times 10^{13}$ kg/y. Further, assuming an Fe–H_2S ratio of ~12:1 and an iron concentration of ~50 mmol Fe/kg (28, 29), we estimate the iron flux to the entire Archean ocean to have been $\sim 4.5 \times 10^{12}$ mol Fe/y. For heuristic purposes, we assume the iron was uniformly dispersed in the ocean, and therefore only ~1% of the flux would have been exposed to UV radiation. Hence, the photooxidative capacity in the photic zone of the Archean ocean would have exceeded the flux of iron by three orders of magnitude. This analysis strongly suggests that virtually all iron in the photic zone was photooxidized during the entire Archean eon.

Since two iron atoms are oxidized for each hydrogen molecule, we can further estimate the global hydrogen production capacity in the early Archean upper ocean to be $\sim 2 \times 10^{10}$ mol H_2/y, which is comparable to the estimated volcanic production rate of $\sim 10^{11}$ mol/y (30). Our experimental results suggest that the photooxidation of siderite during the Archean potentially supplied significant amounts of molecular hydrogen in the upper ocean and to the atmosphere. This reaction would have had important consequences during the first half of Earth's history.

Discussion

Proposed Reaction Mechanism. The results of this study clearly establish that siderite can be readily photooxidized by UV light to generate molecular hydrogen and ferri-oxyhydroxides under anoxic conditions in an aqueous phase. From oxygen K-edge spectroscopy and density functional theory (31), the projected density of states based on hybrid function (B3LYP) revealed an energy gap of 4.6 eV (i.e., 270 nm), corresponding to either the energy between Fe(3d) and a C–O antibonding orbital or, alternatively, between O^{2-} and an Fe^{2+} excitation band gap. We propose that the first photon could produce a charge separation via electron excitation from Fe(3d) state to a C–O antibonding orbital, converting Fe(II)–Fe(II) into Fe(I)–Fe(III). This process would be promoted by simultaneous protonation of the surface Fe(I). The second photon would also produce a charge separation, forming highly reactive hydrido–Fe(III), which subsequently reacts with a proton from solution, giving H_2 and second Fe(III). The production of a H_2 molecule accompanies oxidation and hydrolysis of two Fe(III) atoms, resulting in an iron oxyhydroxide mineral phase. The oxyhydroxide spontaneously is transformed to a magnetic assemblage of magnetite and maghemite. The solid-state transformation from the oxyhydroxide phase to magnetite/maghemite is accompanied by a loss of water molecules and recombination of ferrous iron with ferric iron.

Hydrogen Fueled Early Archean Microbial Community. The photochemically generated flux of hydrogen would have provided a local source of reductant for H_2-utilizating microbial communities in the photic zone of the Archean ocean. This source of hydrogen would have favored the evolution of anoxygenic phototrophs that used the gas as an electron donor for photosynthesis. Indeed, thin, siderite-bearing, carbonaceous laminations preserved in shallow-water facies of the 3.4 Ga Buck Reef Chert, South Africa, have been interpreted to represent some of the oldest known mats constructed by photosynthetic microbes (32, 33) and hydrogen was the most probable electron donor to this ancient microbial community (34, 35). Furthermore, a photochemical source of hydrogen would have provided a vast amount of energy for early chemolithotrophs, such as acetogens and methanogens. Ancient prokaryotic lineages of bacteria and archea that harbored the reductive acetyl–CoA pathway (36), considered one of the earliest bioenergetic metabolisms (37), would have flourished in the photic zone and may have been key members of the microbial photoautotrophic community in the surface waters of the Archean ocean (34, 35).

Solar Radiation Cycles Iron in the Upper Archean Ocean. The photooxidation of siderite in the upper ocean potentially alters our conceptual models of the Archean iron cycle (17). Ubiquitous carbonate minerals, such as diagenetic and ferroan dolomite in the terrestrial and shallow-water settings and siderite in deep-water settings, suggest a carbonate-rich Archean ocean. The paucity of siderite in shallow-water sequences could be the result of low iron flux from deep thermal vents to the upper ocean, but the existence of shallow-water banded-iron formations suggests there must have been a significant source of iron to the upper ocean. With the estimated UV flux through a water column and the corresponding reaction quantum yield, the maximum iron oxidation capacity in the photic zone is $\sim 10^{13}$ mol Fe/y, which is in excess of the optimistic estimation of the total Archean iron flux of $\sim 5 \times 10^{12}$ mol/y into the total ocean from hydrothermal sources. The calculations imply the top 1% of the Archean ocean (i.e., the "photic zone") has a much greater capacity for iron oxidation compared with the net iron flux from hydrothermal vents. We suggest that siderite in the photic zone of the Archean ocean was destroyed by UV radiation, leaving little trace except for iron oxides.

Photochemical Formation of Iron Oxides. The deposition of iron oxides is a hallmark of sedimentary sequences throughout the Archean and Proterozoic eons (38). The iron oxides originate at $\sim 3{,}760 \pm 70$ Ma up to the late Precambrian, however the process (es) responsible for their formation remain enigmatic (39). The primary mineral product of UV photooxidized siderite under anoxic conditions is magnetite, suggesting solar UV radiation may have supplied iron oxides abiologically. Indeed, the deposition of ferric iron is potentially indicative of the UV flux during the Archean.

Photochemical Reactions Alter Planetary Redox State. Hydrogen production from the photooxidation of siderite, and the subsequent escape of the gas from Earth's atmosphere would have altered the oxidation state of the planet (40, 41). This reaction ultimately was attenuated but may not have been entirely quenched by the photobiological production and accumulation of ozone in Earth's atmosphere following the Great Oxidation Event (GOE) at ~2.3 Ga. The generation of ozone clearly would have blocked shorter wavelength UV radiation, and quenched the mass-independent fractionation of sulfur isotopes in SO_2 (42). However, up until that time, the photochemical oxidation of siderite and the loss of hydrogen almost certainly continued unabated. Depending on the ozone concentration, the photochemical oxidation of siderite could have continued for several hundred million years after the GOE, and in the process accelerated the long-term oxidation of Earth's crust and atmosphere.

The photochemistry of siderite and potentially other Earth-abundant minerals in shaping the biogeochemistry of Earth is a poorly explored area of experimental geochemistry, which we call "photogeochemistry." Our experimental results strongly suggest that the photochemical oxidation of an abundant mineral potentially generated a significant source of hydrogen in shallow waters of the Archean oceans for several hundred million years, if not longer. The reaction would have continued through the Archean

to at least the early phases of the GOE, and provided a mechanism for oxidizing the planet through the abiotic production of hydrogen and its loss of hydrogen to space, while simultaneously providing a key reductant for microbial metabolism. This process may have operated on Mars when it was a wet planet, and should be operating on other terrestrial planets with liquid water in the habitable zone, as long as they do not have gases that greatly attenuate UV photons from their stars.

Methods

Siderite Synthesis. Siderite was synthesized by mixing solutions of $FeSO_4$ and Na_2CO_3 under anoxic condition (1% H_2/N_2 gas mixture) in a glovebox. Sulfate and sodium ions in the siderite precipitate solution were removed by repeated washing with deoxygenated Milli-Q water. The siderite was filter dried under N_2, transferred to a capillary tube and sealed for analysis with a transmission XRD technique to confirm the product (Fig. S2). Upon exposure to oxygen, siderite becomes the nonmagnetic mineral, goethite (Fig. S3).

Optical Setup. All components were installed on a Newport optical bench (Fig. S4). A 1,000 W Xe source (Oriel/Newport) was used throughout the experiments. A water filter was installed, and water was circulated to prevent heat transfer from the source, and a collimator was attached at the end of the water filter. Three bandpass filters were used to isolate the UV source with centers at 260, 270, and 280 nm. A fiber optics spectrometer (Ocean Optics USB 4000) was used to characterize the spectral irradiance of the source (from 200 to 800 nm at 0.22 nm resolution) (Fig. S5).

Siderite Photooxidation and Analysis. A quartz reaction vessel with stress-relief gratings was fused with a serum bottle for the experiment. The final internal volume was ~75 mL and 3 mL of siderite suspension (~44 μmol $FeCO_3$), and 22 mL of boiled, anoxic Milli-Q water was transferred to the custom-made quartz reaction vessel in a glovebox. The sealed quartz tube was purged with ultra-high-purity N_2 gas for 10 min to ensure the absence of hydrogen or oxygen inside the tube. The headspace (50 mL) was analyzed by gas chromatography (SRI Instruments) with a thermal conductivity detector (Fig. S6). To confirm that the gas produced by UV photooxidation was hydrogen, a membrane-inlet quadrupole mass spectrometer was used and the signal for *m/z* of 2 was recorded.

Ferrioxalate Chemical Actinometry. To measure the number of incident photons, we used a ferrioxalate chemical actinometer (43).

ACKNOWLEDGMENTS. We thank Fraser Armstrong and Piotr Piotrowiak for insightful discussions on the reaction mechanism; Silke Severmann, Robert Kopp, and Donald Lowe for critical discussions on Archean iron cycles; David Mauzerall, Maxim Gorbunov, and Fedor Kuzminov for helpful discussions on photochemistry; Tom Emge and YongBok Go for X-ray analyses; and Kevin Wyman for discussions and technical assistance. This research was supported by National Science Foundation Grant 0940187 (to P.G.F., N.Y., and V.N.).

1. Oparin AI (1957) Chapter I. Theories of the spontaneous generation of life. *The Origin of Life on the Earth*, 3rd Ed (Academic Press Inc. New York).
2. Kim JD, Rodriguez-Granillo A, Case DA, Nanda V, Falkowski PG (2012) Energetic selection of topology in ferredoxins. *PLOS Comput Biol* 8(4):e1002463.
3. Hazen RM, Sverjensky DA (2010) Mineral surfaces, geochemical complexities, and the origins of life. *Cold Spring Harb Perspect Biol* 2(5):a002162.
4. Da Silva JF, Williams RJP (2001) *The Biological Chemistry of the Elements: The Inorganic Chemistry of Life* (Oxford Univ Press, New York).
5. Marcus RA (1965) On the theory of electron transfer reactions. VI. Unified treatment for homogeneous and electrode Reactions. *J Chem Phys* 43(2):679–701.
6. Falkowski PG, Fenchel T, Delong EF (2008) The microbial engines that drive Earth's biogeochemical cycles. *Science* 320(5879):1034–1039.
7. Wordsworth R, Pierrehumbert R (2013) Hydrogen-nitrogen greenhouse warming in Earth's early atmosphere. *Science* 339(6115):64–67.
8. Canfield DE, Rosing MT, Bjerrum C (2006) Early anaerobic metabolisms. *Philos Trans R Soc Lond B Biol Sci* 361(1474):1819–1834, discussion 1835–1836.
9. Borowska Z, Mauzerall D (1986) Formation of hydrogen on irradiation of aqueous ferrous ion with UV-light at neutral pH. *Orig Life Evol Biosph* 16(3-4):194–195.
10. Borowska ZK, Mauzerall DC (1987) Efficient near ultraviolet light induced formation of hydrogen by ferrous hydroxide. *Orig Life Evol Biosph* 17(3-4):251–259.
11. Braterman P, Cairns-Smith AG, Sloper RW (1983) Photo-oxidation of hydrated Fe^{2+}–significance for banded iron formations. *Nature* 303(5913):163–164.
12. Cairns-Smith AG (1978) Precambrian solution photochemistry, inverse segregation, and banded iron formations. *Nature* 276(5690):807–808.
13. Holland HD (2003) The geological history of seawater. *Treatise on Geochemistry*, eds Holland HD, Turekian KK (Elsevier, Oxford, UK), pp 583–625.
14. Konhauser KO, et al. (2007) Decoupling photochemical Fe(II) oxidation from shallow-water BIF deposition. *Earth Planet Sci Lett* 258(1-2):87–100.
15. Kasting JF (1993) Earth's early atmosphere. *Science* 259(5097):920–926.
16. Jensen DL, Boddum JK, Tjell JC, Christensen TH (2002) The solubility of rhodochrosite ($MnCO_3$) and siderite ($FeCO_3$) in anaerobic aquatic environments. *Appl Geochem* 17(4):503–511.
17. Klein C (2005) Some Precambrian banded iron-formations (BIFs) from around the world: Their age, geologic setting, mineralogy, metamorphism, geochemistry, and origin. *Am Mineral* 90(10):1473–1499.
18. Klein C, Beukes NJ (1989) Geochemistry and sedimentology of a facies transition from limestone to iron-formation deposition in the early Proterozoic Transvaal Supergroup, South-Africa. *Econ Geol* 84(7):1733–1774.
19. Hessler AM, Lowe DR, Jones RL, Bird DK (2004) A lower limit for atmospheric carbon dioxide levels 3.2 billion years ago. *Nature* 428(6984):736–738.
20. Kaufman AJ, Hayes JM, Klein C (1990) Primary and diagenetic controls of isotopic compositions of iron-formation carbonates. *Geochim Cosmochim Acta* 54(12): 3461–3473.
21. Ohmoto H, Watanabe Y, Kumazawa K (2004) Evidence from massive siderite beds for a CO2-rich atmosphere before approximately 1.8 billion years ago. *Nature* 429(6990): 395–399.
22. Joe H, Kuma K, Paplawsky W, Rea B, Arrhenius G (1986) Abiotic photosynthesis from ferrous carbonate (siderite) and water. *Orig Life Evol Biosph* 16(3-4):369–370.
23. Cockell CS, Raven JA (2007) Ozone and life on the Archaean earth. *Philos T R Soc A* 365(1856):1889–1901.
24. Morel A, Smith RC (1974) Relation between total quanta and total energy for aquatic photosynthesis. *Limnol Oceanogr* 19(4):591–600.
25. Smith RC, Baker KS (1981) Optical properties of the clearest natural waters (200-800 nm). *Appl Opt* 20(2):177–184.
26. Elderfield H, Schultz A (1996) Mid-ocean ridge hydrothermal fluxes and the chemical composition of the ocean. *Annu Rev Earth Planet Sci* 24:191–224.
27. Isley AE (1995) Hydrothermal plumes and the delivery of iron to banded iron formation. *J Geol* 103(2):169–185.
28. Kump LR, Seyfried WE (2005) Hydrothermal Fe fluxes during the Precambrian: Effect of low oceanic sulfate concentrations and low hydrostatic pressure on the composition of black smokers. *Earth Planet Sci Lett* 235(3):654–662.
29. Shibuya T, Komiya T, Nakamura K, Takai K, Maruyama S (2010) Highly alkaline, high-temperature hydrothermal fluids in the early Archean ocean. *Precambrian Res* 182(3): 230–238.
30. Tian F, Toon OB, Pavlov AA, De Sterck H (2005) A hydrogen-rich early Earth atmosphere. *Science* 308(5724):1014–1017.
31. Sherman DM (2009) Electronic structures of siderite ($FeCO_3$) and rhodochrosite ($MnCO_3$): Oxygen K-edge spectroscopy and hybrid density functional theory. *Am Mineral* 94(1):166–171.
32. Tice MM, Lowe DR (2004) Photosynthetic microbial mats in the 3,416-Myr-old ocean. *Nature* 431(7008):549–552.
33. Tice MM, Lowe DR (2006) Hydrogen-based carbon fixation in the earliest known photosynthetic organisms. *Geology* 34(1):37–40.
34. Lovley DR, Phillips EJP, Lonergan DJ (1989) Hydrogen and formate oxidation coupled to dissimilatory reduction of iron or manganese by *Alteromonas Putrefaciens*. *Appl Environ Microbiol* 55(3):700–706.
35. Mojzsis SJ, et al. (1996) Evidence for life on Earth before 3,800 million years ago. *Nature* 384(6604):55–59.
36. Ljungdahl LG (1986) The autotrophic pathway of acetate synthesis in acetogenic bacteria. *Annu Rev Microbiol* 40:415–450.
37. Braakman R, Smith E (2012) The emergence and early evolution of biological carbon-fixation. *PLOS Comput Biol* 8(4):e1002455.
38. Kump LR, Holland HD (1992) Iron in Precambrian rocks: Implications for the global oxygen budget of the ancient Earth. *Geochim Cosmochim Acta* 56(8):3217–3223.
39. Dymek RF, Klein C (1988) Chemistry, petrology and origin of banded iron-formation lithologies from the 3800-Ma Isua Supracrustal Belt, West Greenland. *Precambrian Res* 39(4):247–302.
40. Walker JCG (1977) *Evolution of the Atmosphere* (Macmillan Pub Co., New York).
41. Catling DC, Zahnle KJ, McKay CP (2001) Biogenic methane, hydrogen escape, and the irreversible oxidation of early Earth. *Science* 293(5531):839–843.
42. Farquhar J, Bao H, Thiemens M (2000) Atmospheric influence of Earth's earliest sulfur cycle. *Science* 289(5480):756–759.
43. Hatchard CG, Parker CA (1956) A new sensitive chemical actinometer. II. Potassium ferrioxalate as a standard chemical actinometer. *Proc R Soc Lond A* 235:518–536.